

# Characterization of order-to-chaos-to-order transition in co-axial DC discharge plasma of different inter-electrode distances

Rahul Kumar<sup>1,\*</sup>, Ramesh Narayanan<sup>2</sup>, R. D. Tarey<sup>1</sup> and Awadhesh Prasad<sup>3</sup>

<sup>1</sup>Department of Physics, Indian Institute of Technology Delhi, Hauz Khas, New Delhi-110016, India

<sup>2</sup>Centre for Energy Studies, Indian Institute of Technology Delhi, Hauz Khas, New Delhi-110016, India

<sup>3</sup>Department of Physics and Astrophysics, University of Delhi, Delhi-110007, India

This paper attempts to understand the role of the electrode dimensions in the evolution of order-to-chaos-to-order transitions in a co-axial DC electrode discharge system, wherein the ratio of the anode-to-cathode radii is observed to determine the evolution path of the transition. Further the anode dimensions is observed to determine the discharge conductivity after the 1<sup>st</sup> negative differential resistance (NDR) region and the onset of the order-to-chaos-to-order transition is linked to the cathode dimensions.

## 1. Introduction

Plasma discharges being a nonlinear medium, observations of associated hysteresis effects at negative differential regions (NDR) are signatures of the nonlinear dynamical evolution of the system. Such hysteresis loops are quite commonly observed near the Townsend breakdown and abnormal glow discharge regions of a planar electrode DC plasma discharge. However, there have also been observations of NDR regions in discharge current ( $I_d$ ) – discharge voltage ( $V_d$ ) characteristics of systems such as the DP machine [1] and coaxial electrode geometry systems [2, 3], in which the dynamical evolution of the system has been characterized using fluctuation signals [2-6] obtained from the plasma. In different systems and under different operating conditions, the fluctuation signals have been observed to undergo order-to-chaos [7] as well as chaos-to-order [8, 9] transitions. Order-to-chaos-to-order transitions [3, 10] have also been observed recently.

As reported earlier, the  $I_d$ - $V_d$  characteristics [3] of the DC coaxial electrode discharges with a powered central anode have been observed to have two consecutive negative differential regions (NDR). The 1<sup>st</sup> NDR has been observed to be correlated to an upper voltage threshold whereas the 2<sup>nd</sup> NDR is seen to be linked to the discharge current [11]. The voltage drop across the 1<sup>st</sup> NDR is seen to trigger relatively large amplitude floating potential oscillations in comparison to those prior to the 1<sup>st</sup> NDR region. These oscillations, thereafter, are seen to undergo an order-to-chaos-to-order transition with increasing discharge current. As the  $I_d$ - $V_d$  characteristic behaviour seems to be linked to the polarity direction of the electrode configuration, the

role of the dependence on the electrode geometry seems to be an important factor. Keeping this in mind, it was envisaged to carry out a study of the discharge characteristics of the co-axial electrode geometry with different inter-electrode distances, by varying the diameters of the anode/cathode.

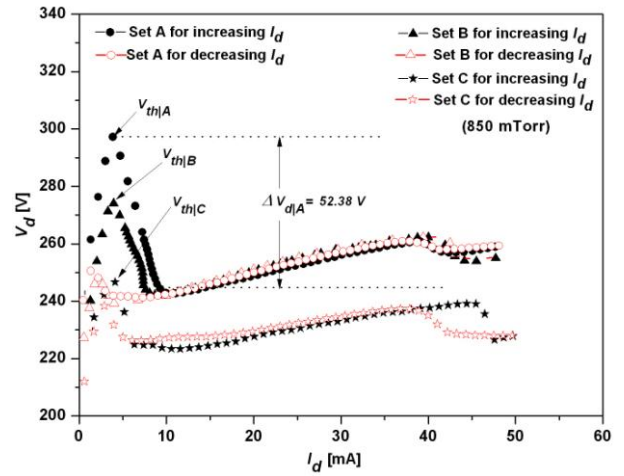


Fig 1:  $I_d$ - $V_d$  discharge characteristics for increasing (black) and decreasing (red)  $I_d$  for different inter-electrode distances at  $p=850$  mTorr.  $V_{th|A}$ ,  $V_{th|B}$  and  $V_{th|C}$  are the threshold voltages at 1<sup>st</sup> NDR for Set A, B & C respectively.  $\Delta V_{d|A}$  is the voltage drop across the 1<sup>st</sup> NDR for Set A.

In this paper, the variation of the order-to-chaos-to-order transitions in the floating potential fluctuations with configurations of different inter-electrode distances are presented and characterized. The characterization has been done with new electrode installed [12]. Thus the characteristics are slightly different as compared to that expressed for longer duration [3, 11].

## 2. Experimental Results and Discussions

The experimental setup [3] consists of a coaxial stainless steel electrode system ( $\approx 60$  mm long), with central axial rod acting as the powered anode and the outer cylindrical tube (thickness  $\approx 1$  mm) acting as the grounded cathode. In this paper, experiments have been carried out with central anode diameters of 1.5 mm and 12 mm and inner diameters of the grounded cathode being 50 mm and 70 mm. Experimental results from three different inter-electrode distances [viz., (1.5, 50), (1.5, 70)

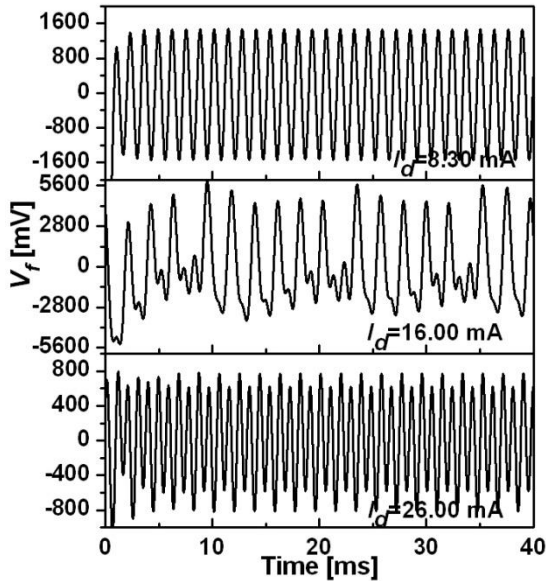


Fig 2: Floating potential oscillations for increasing discharge current for Set A at  $p=850$  mTorr.

and (12, 70)] with an anode to cathode radii ratio of (1/33), (1/47) and (1/6) respectively are presented in this paper. The three configurations are henceforth called Set A, Set B and Set C respectively. A single Langmuir probe has been used for plasma parameter radial profile measurements at an operating pressure of 850 mTorr.

Figure 1 shows the  $I_d$ - $V_d$  characteristics, both for increasing and decreasing currents, for the three different inter electrode distances. The voltage threshold voltage ( $V_{th}$ ) at which the 1<sup>st</sup> NDR occurs is seen to decrease with an increase in the cathode/anode diameters, with the threshold dropping from 297 V to 273 V to 250 V in Set A, B and C electrode configurations respectively. It is interesting to note that the discharge current at which the 1<sup>st</sup> NDR is triggered is the same ( $\sim 3.5$  mA). The dominant effect is observed when the anode rod diameter is increased. The voltage drop

( $\Delta V_d$ ) across the 1<sup>st</sup> NDR is seen to decrease from 53 V to 35 V to 25 V. It is further observed that the conductivity of the system after the first NDR seems to increase with change in the central anode diameter, as seen by the sustenance of the discharge at a lower discharge voltage for Set C configuration, which however, does not seem to change much for Set A and Set B.

The region between the 1<sup>st</sup> NDR and 2<sup>nd</sup> NDR is seen to undergo an order-to-chaos-to-order transition [3, 11] in the floating potential oscillations in all three sets. Similar features have been observed for all the different electrode configurations reported here. However, the regions of onset of this transition and their behaviour are not same for all the configurations. Figs. 2, 3 and 4; show three representative oscillations, for each of the Sets A, B & C, depicting an order-to-chaos-to-order transition as one increases  $I_d$ . It is to be noted that oscillations at other  $I_d$ 's have also been recorded but not shown here.

For Set A, it is observed that after the 1<sup>st</sup> NDR, the oscillations have an ordered behaviour from  $I_d \approx 8.34$  mA to 15.9 mA whereas the chaotic zone is from  $I_d \approx 16.0$  mA to 18.0 mA. Thereafter the oscillations remain ordered up to the maximum discharge current (46.0 mA) recorded.

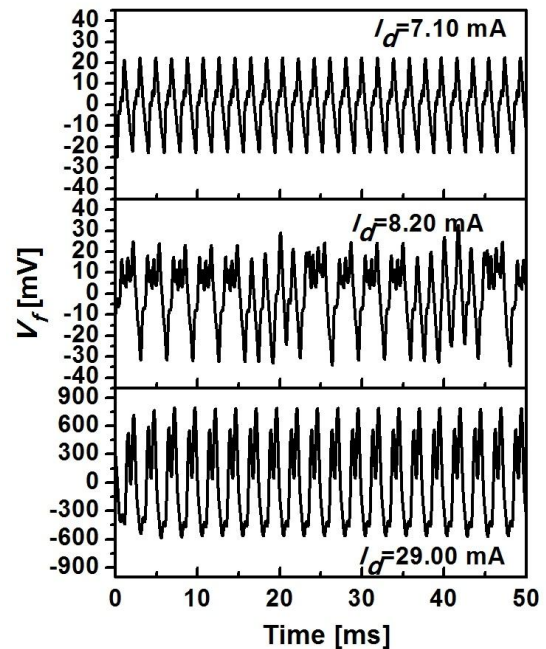


Fig 3: Floating potential oscillations for increasing discharge current for Set B at  $p=850$  mTorr.

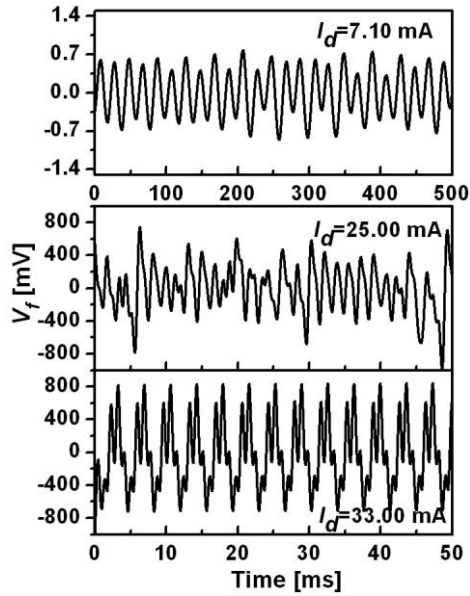


Fig. 4: Floating potential oscillations for increasing discharge current for Set C at  $p=850$  mTorr.

For Set B, the oscillations show order at  $I_d \approx 7.10$  mA, just after the 1<sup>st</sup> NDR. These remain ordered up to 8.10 mA of  $I_d$  value. The chaotic zone is observed to widen from  $I_d \approx 8.20$  mA to 28.8 mA. The oscillations at  $I_d \approx 29.0$  mA is observed to be ordered. At  $I_d \approx 31.10$  mA and  $I_d \approx 33.0$  mA, the system again becomes chaotic. At  $I_d \approx 35.5$  mA, it is ordered again. At  $I_d \approx 37.0$  mA to 42.0 mA, the system is chaotic. As the control parameter limit is reached, the system becomes ordered again (i.e. between  $I_d \approx 42.8$  mA to 45.0 mA). Thus it is seen that in this configuration, the system traverses the order-chaos-order path again and again.

In Set C, the oscillations depict order in the current range  $I_d \approx 7.10$  mA to 24.5 mA whereas from  $I_d \approx 25.0$  mA to 29.0 mA, it is chaotic and thereafter at higher  $I_d$ 's, the system tends to become ordered as  $I_d$  is increased to 48.0 mA.

#### 4. Characterization of the Fluctuations

The onset of the chaos-order-chaos region and its evolution pattern seems different and thus a basic characterization of these fluctuations were carried out with respect to  $I_d$ . The amplitude bifurcation of the oscillations shown in Fig. 5 for Sets A, B and C show that the onset of the chaotic region starts at higher and higher  $I_d$  values as one shows from Set A to Set B to Set C configurations respectively. The current jump is more significant from Set A to Set B. Further, the behaviour of the bifurcation diagram seems to evolve differently in the three cases, with the system tending to become

ordered more slowly when the inter electrode distance is maximum (Set B).

The amplitude levels also show an interesting trend. As seen in Set B of Fig. 5, at  $I_d \approx 21.3$  mA, the amplitude of oscillations suddenly increase and tends to remain in this increased level up to  $I_d \approx 31.10$  mA. Thereafter at  $I_d \approx 33.0$  mA, the amplitude levels of oscillations show a decreasing trend till the control parameter limit. Comparing this with Set A and Set C, one finds in these sets that the large amplitude phenomenon tends to decrease relatively

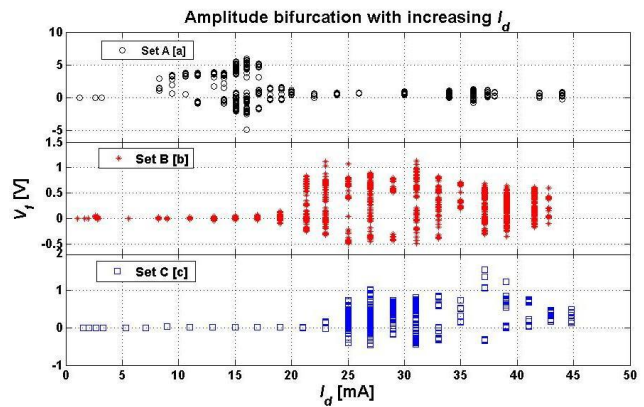


Fig. 5: Amplitude bifurcation diagram from the different electrode dimensions at  $p=850$  mTorr: (a) Set A, (b) Set B, and (c) Set C.

faster after a certain current limit with the amplitudes remaining at lower levels ( $\sim 20$  mV). Thereafter, the amplitude decay rate is slightly slower in Set C as compared to Set A. It may be possible that one observes such reduction in amplitude levels at higher  $I_d$  in Set B also but at present the experimental set up does not have the facility to go to such high discharge currents.

In order to understand the deviation of the oscillations from the DC level, their variance has been estimated (Fig. 6) which reveals that the variance is large in the region of the chaotic regions and hence onset of maximum variance tends to shift to the right i.e. linked to the onset of the order-to-chaos-to-order transition with the largest shift being observed when the cathode diameter is changed (i.e. Set A to Set B/C) as observed in Fig. 5 also.

#### 3. Conclusions

The changes in the onset of the 1<sup>st</sup> NDR when one characterizes Set A, Set B and Set C configuration; show that the NDR is triggered at significantly higher conductivity as the electrode

surface area is increased and the system transits to a significantly higher conducting state after 1<sup>st</sup> NDR

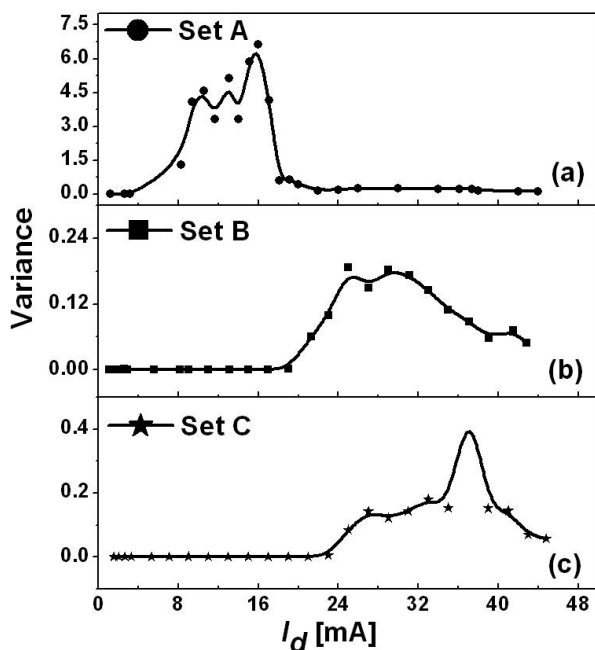


Fig. 6: Variance versus  $I_d$  for the different electrode dimensions at  $p = 850$  mTorr: (a) Set A, (b) Set B, and (c) Set C.

when the anode diameter is changed. However, the onset of the order-to-chaos-to-order transition seems to be governed by the cathode dimensions. Further it needs to be stated that the evolution of the order-to-chaos-to-order zone seems dependent on a critical value of the ratio of anode-to-cathode radii which needs to be investigated further.

#### 4. References

- [1] C. Ionita, D. G. Dimitriu, and R. W. Schrittwieser, *Int. J. Mass. Spectrom.* **233** (2004) 343.
- [2] Md. Nurujjaman, R. Narayanan, and A. N. S. Iyengar, *Chaos* **17** (2007) 043121
- [3] R. Kumar, R. Narayanan and A. Prasad, *Phys. Plasmas* **21** (2014) 123501.
- [4] Md. Nurujjaman and A. N. S. Iyengar, *Phy. Lett A* **360** (2007) 717.
- [5] Md. Nurujjaman, R. Narayanan, and A. N. S. Iyengar, *Phys. Plasmas* **16** (2009) 102307.
- [6] S. Gurlui, D. G. Dimitriu, C. Ionita, and R. W. Schrittwieser, *Rom. Journ. Phys.* **54** (2009) 705.
- [7] V. Mitra, A. Sarma, M.S. Janaki, A.N. Sekar Iyengar, B. Sarma, N. Marwan, J. Kurths, P. K.

Shaw, D. Saha, S. Ghosh, *Chaos, Solitons & Fractals*, **69**, (2014), 285.

[8] S. Lahiri, D. Roychowdhury, and A. N. S. Iyengar, *Phys. Plasmas* **19** (2012) 082313.

[9] Md. Nurujjaman and A. N. S. Iyengar, *Pramana, J. Phys.* **67** (2006) 299.

[10] M. Agop, D. G. Dimitriu, L. Vrajitoriu, and M. Boicu, *J. Phys. Soc. Jpn.* **83** (2014) 054501.

[11] R. Narayanan, R. Kumar, R. D. Tarey, A. Ganguli, Proceedings of PPPS-2013 held in San Francisco, California, USA from June 16-21, 2013, Publ. IEEE & POD Publ. Curran Associates, Inc. ISBN: 978-1-4673-5166-9, **1**, (2014) 435.

[12] R. Narayanan, R. Kumar, R. D. Tarey, A. Ganguli, "Hysteresis Flip Effects On the DC Plasma Discharge Characteristics Of A Co-Axial Electrode Geometry", Submitted to XXXII International Conference on Phenomenon in Ionized Gases, July 26-31, 2015, Iasi, Romania.